Surface functionalization of thin-film diamond for highly stable and selective biological interfaces

Courtney Stavis[a], Tami Lasseter Clare[a,2], James E. Butler[b], Adarsh D. Radadia[c,d], Rogan Carr[e], Hongjun Zeng[f], William P. King[d,g], John A. Carlisle[f], Aleksei Aksimentiev[e], Rashid Bashir[c,d,h], and Robert J. Hamers[a,1]

[a]Department of Chemistry, University of Wisconsin at Madison, 1101 University Avenue, Madison, WI 53706; [b]U.S. Naval Research Laboratory, 4555 Overlook Avenue, SW Washington, DC 20375; [c]Department of Electrical and Computer Engineering, University of Illinois, Urbana, IL 61801; [d]Micro and Nano Technology Laboratory, University of Illinois, Urbana, IL 61801; [e]Department of Physics, University of Illinois, Urbana, IL 61801; [f]Advanced Diamond Technologies, Inc., 429 B Weber Road #286, Romeoville, IL 60446; [g]Department of Mechanical Science and Engineering, University of Illinois, Urbana, IL 61801; and [h]Department of Bioengineering, University of Illinois, Urbana, IL 61801

Edited by Charles T. Campbell, University of Washington, Seattle, WA, and accepted by the Editorial Board August 12, 2010 (received for review June 6, 2010)

Carbon is an extremely versatile family of materials with a wide range of mechanical, optical, and mechanical properties, but many similarities in surface chemistry. As one of the most chemically stable materials known, carbon provides an outstanding platform for the development of highly tunable molecular and biomolecular interfaces. Photochemical grafting of alkenes has emerged as an attractive method for functionalizing surfaces of diamond, but many aspects of the surface chemistry and impact on biological recognition processes remain unexplored. Here we report investigations of the interaction of functionalized diamond surfaces with proteins and biological cells using X-ray photoelectron spectroscopy (XPS), atomic force microscopy, and fluorescence methods. XPS data show that functionalization of diamond with short ethylene glycol oligomers reduces the nonspecific binding of fibrinogen below the detection limit of XPS, estimated as >97% reduction over H-terminated diamond. Measurements of different forms of diamond with different roughness are used to explore the influence of roughness on nonspecific binding onto H-terminated and ethylene glycol (EG)-terminated surfaces. Finally, we use XPS to characterize the chemical stability of *Escherichia coli* K12 antibodies on the surfaces of diamond and amine-functionalized glass. Our results show that antibody-modified diamond surfaces exhibit increased stability in XPS and that this is accompanied by retention of biological activity in cell-capture measurements. Our results demonstrate that surface chemistry on diamond and other carbon-based materials provides an excellent platform for biomolecular interfaces with high stability and high selectivity.

biointerfaces | surface chemistry | cells

Biological recognition is a complex phenomenon that can involve multiple types of short-range, long-range, and dynamic interactions. The interaction of proteins with solid surfaces is of importance in many applications, such as medical implants, (1, 2) biosensors (3–5), and in vivo drug delivery devices (6). The controlled adsorption of proteins to surfaces plays a crucial role in the adhesion of cells to surfaces (7) and is an area of intense research in stem-cell research (8, 9) and biosensor development (4, 10, 11). Conversely, uncontrolled adsorption of proteins can induce a range of adverse phenomena such as fouling of biosensors and initiation of inflammatory response from implants (7, 12).

Self-assembled monolayers (SAMs) of alkanethiols on gold have emerged as a model system for investigating biological interactions at surfaces because SAMs provide an extremely versatile platform for investigating surface chemical functionalization (6, 13–18). One outcome of these prior studies has been to demonstrate that alkanethiols bearing even very short ethylene glycol (EG) groups can drastically reduce nonspecific binding of proteins (6, 13–18). Yet, while gold-thiol SAM chemistry is an excellent model system, it suffers from chemical instabilities that limit its actual application (16, 19). These instabilities have, in turn, lead to increased interest in alternative system that can provide higher stability.

Carbon-based surfaces, such as diamond, glassy carbon, and diamond-like carbon, are attractive substrates for biological interfaces because of their biocompatibility, mechanical hardness, and because they are extraordinarily chemically robust, resembling in many ways the properties of organic alkanes (20, 21). While the surface chemistry of carbon is relatively unexplored, in recent work we have shown that photochemical grafting of organic alkenes can provide an extremely robust way to link functional organic molecules to surfaces of carbon, including diamond (22–26), amorphous carbon (23, 27, 28), glassy carbon (29), and carbon nanofibers (30, 31). Carbon surfaces functionalized in this manner have shown excellent stability, even at elevated temperatures (32). Of the various forms of carbon, diamond and diamond-like carbon (DLC) are of particular interest because diamond's unique role as the hardest natural material makes it of interest for possible application as a thin-film coating material for biomedical implants such as prosthetic devices. DLC thin films provide NiTi alloys (commonly used as an implant material) with improved corrosion resistance (33) and reduce leaching of Ni (34). Empirical evidence shows that carbon-based materials exhibit little inflammatory response (35) and exhibit high stability as substrates for biosensing (4, 31), but the relationships between substrate roughness, protein adsorption, and stability are poorly understood.

Here we report investigations of the use of photochemical grafting methods to link highly stable, functional molecular layers to diamond films in order to control the resulting interactions with proteins. We demonstrate the influence of surface chemistry and roughness on nonspecific binding of proteins. Finally, we show that these grafting methods can produce antibody-modified surfaces that exhibit enhanced stability and extended biological activity toward biological cells.

Results

Reproducible surfaces of diamond and diamond-like carbons can be prepared by exposure to atomic hydrogen, which removes oxidized sites and leaves surface atoms terminated with hydrogen atoms (36). As depicted in Fig. 1, organic alkenes will graft to the resulting H-terminated surfaces when illuminated with UV light

Author contributions: C.S., T.L.C., A.D.R., R.B., and R.J.H. designed research; C.S., T.L.C., and A.D.R. performed research; J.E.B., R.C., H.Z., W.K., J.A.C., A.A., R.B., and R.J.H. contributed new reagents/analytic tools; C.S., T.L.C., A.D.R., R.C., R.B., and R.J.H. analyzed data; and C.S., T.L.C., and R.J.H. wrote the paper.

Conflict of interest statement: Hongjun Zeng and John A.Carlisle have a financial interest in Advanced Diamond Technologies, which funded this work through a subcontract from the Defense Threat Reduction Agency.

This article is a PNAS Direct Submission. C.T.C. is a guest editor invited by the Editorial Board.

[1]To whom correspondence should be addressed. E-mail: rjhamers@wisc.edu.

[2]Present address: Department of Chemistry, Portland State University, Portland, OR 97207.

This article contains supporting information online at www.pnas.org/lookup/suppl/doi:10.1073/pnas.1006660107/-/DCSupplemental.

at 254 nanometer (nm). Fig. 1*B* shows some specific molecules of particular interest for biologically modified surfaces: molecules bearing ethylene glycol groups (EG6) and protected amine groups (TFAAD) are of interest because these form biological interfaces that can resist proteins (EG6) and can serve as attachment points for proteins and other biomolecules of interest (TFAAD). 1-dodecene can be used to control the spacing between functional groups through the formation of mixed monolayer. The detailed mechanism of grafting on diamond has been elucidated (24, 25) and is illustrated in Fig. 1*C*. The grafting reaction is initiated by UV-induced photoemission of electrons, which is facilitated by the presence of electron-acceptor groups in the reactant liquid or pregrafted onto the surface (37). The photoemission process creates positively charged, carbocation-like surface sites (24). Nucleophilic attack by the electron-rich alkene group then grafts the molecules to the diamond surface. Experimental and computational results show that reactivity of different alkenes correlates with the electron affinity of the "R" group (24, 28, 38).

Molecular Monolayers to Resist Protein Binding. Previous studies of protein-resistant monolayers have focused primarily on self-assembled monolayers on gold (6, 13–18) or silane chemistry (16, 39). We recently used fluorescence methods to show that EG6 oligomers bound to diamond surfaces were also highly effective at resisting protein binding (26, 40). However, comparisons of different materials or different morphologies are difficult to quantify by this approach because fluorescence quenching can vary substantially between different substrates. In some cases wash-off methods can be used to remove the protein from the surface (*vide infra*) (40) but this is not feasible with many proteins. To evaluate the ability of EG6-functionalized diamond to resist protein binding, we conducted XPS studies of H-terminated and EG6-modified diamond samples before and after exposure to fibrinogen. Fig. 2 shows C(1s), N(1s), and S(2p) XPS spectra of H-terminated diamond thin films (blue), EG6-functionalized diamond thin films (green), and spectra of a thick film of fibrinogen deposited on a planar Si substrate (red). The spectra of diamond are shown before and after exposure to fibrinogen.

The XPS spectra of the pure fibrinogen multilayer film are consistent with those reported previously (41), showing multiple C(1s) peaks and significant intensity in the N(1s) and S(2p) regions. The C(1s) peak at 288.2 eV arises from carbon atoms in the amide groups (41). The N(1s) region shows a single sharp peak, while the S(2p) spectrum shows two peaks that reflect nonoxidized (163 eV) and oxidized (168 eV) forms of sulfur in cysteine

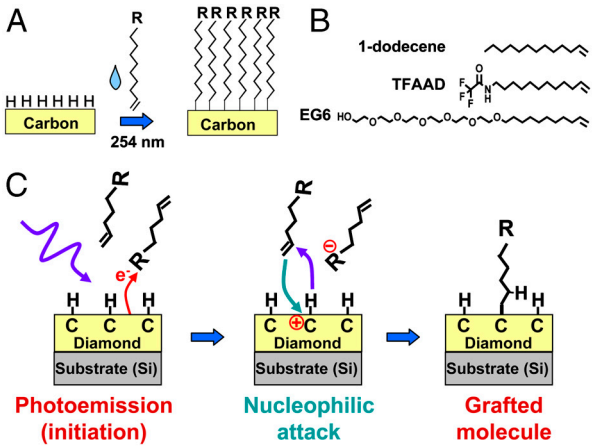

Fig. 1. *A*) Photochemical grafting of alkenes to H-terminated surfaces of carbon. *B*) Molecules used in the work presented here *C*) Simplified mechanism of photochemical grafting to surfaces of diamond and other forms of carbon.

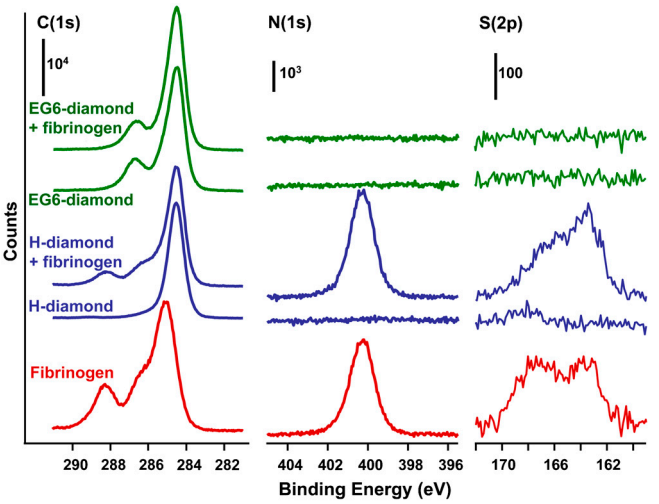

Fig. 2. XPS spectra of H-terminated and EG6-functionalized surfaces of NCD film. The bottom spectrum shows the XPS spectrum of a thick film of fibrinogen. The diamond spectra are depicted on an absolute counts scale to facilitate comparison of intensities. The spectra of the fibrinogen film were scaled separately.

and methionine residues. The H-terminated ultrananocrystalline diamond (UNCD) sample shows a single sharp C(1s) peak and no measureable intensity in the N(1s) or S(2p) regions. After grafting of EG6 the sample shows two C(1s) peaks: one at 284.5 eV from the diamond substrate and the EG6 alkyl chain, and one at 286.7 eV from the C atoms within the EG part of the molecule.

After immersion in fibrinogen solution, the C(1s) spectrum of H-terminated diamond shows clear increases in the C(1s), N(1s), and S(2p) peak intensities. In contrast, the EG6-modified diamond sample shows no detectable increase beyond the experimental noise level. Based on the signal-to-noise of the N(1s) data, we estimate that our detection limit from XPS corresponds to ~3% of the N(1s) signal produced by fibrinogen adsorbed onto H-terminated sample. Thus, we conclude that photochemical grafting of EG6 to diamond surfaces reduces nonspecific binding of fibrinogen by >97% compared with that of the H-terminated surface.

Protein-Resistant Carbon Surfaces: the Role of Surface Roughness. To understand how roughness influences nonspecific binding of proteins on H-terminated and EG6-functionalized diamond, we explored three types of samples: (*i*) a nanocrystalline diamond thin-film (NCD), (*ii*) a polished synthetic diamond (PD), and (*iii*) a (111)-oriented cleavage face of a large natural single-crystal diamond (SCD). These substrates ranges from atomically flat (SCD) to surfaces comprised of rough assemblies of randomly oriented nanocrystals (NCD), spanning an rms roughness between 5 nm and 0.2 nm.

For these measurements we used avidin as a model system because of its simpler morphology (compared with the highly elongated and variable structure of fibrinogen, for example) and because in previous work we validated the use of a fluorescence wash-off method to quantify the nonspecific binding of avidin (40). After exposing the surface of interest to fluorescently labeled avidin under a given set of conditions the nonspecifically adsorbed material can be digested and released from the surface into solution for quantitative fluorescence measurements. This procedure avoids problems of surface-initiated fluorescence quenching. Complete removal from the surface during the digestion can be easily validated experimentally (40).

Fig. 3 shows AFM images and height profiles for each sample investigated before (Fig. 3 *A* and *B*) and after (Fig. 3 *C* and *D*) grafting EG6 onto the surfaces. From analysis of AFM images, we

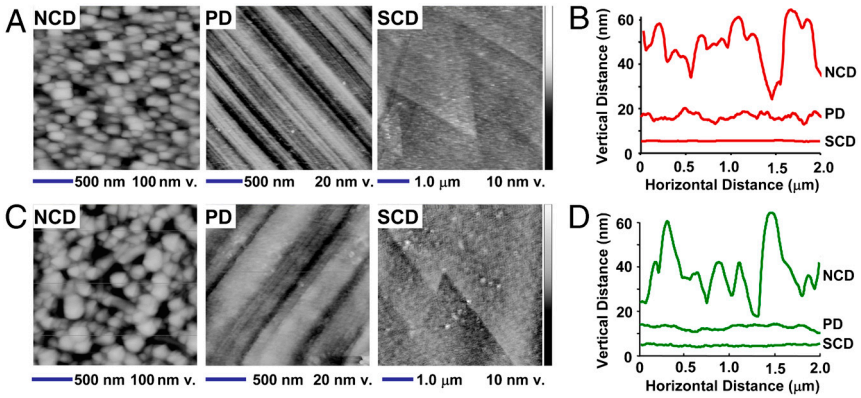

Fig. 3. Comparison of roughness and nonspecific binding of avidin on different forms of diamond. Data shown are for a NCD thin-film, a PD crystal, and a cleaved natural single-crystal cleaved along the (111) face (SCD). *A*) AFM images of H-terminated diamond samples before functionalization with EG6. Note the greatly exaggerated vertical scale. *B*) Height profiles of H-terminated diamond samples. *C*) AFM images of H-terminated diamond samples after functionalization with EG6. *D*) Height profiles of diamond samples after functionalization with EG6.

also calculated the root-mean-square surface roughness, shown in Fig. 4*A*. NCD has a continuous surface composed of crystalline diamond grains ~100 nm in width and 50 nm in height and an rms roughness of 5.1 nm. PD is smoother but has many finely spaced scratches (visible as parallel lines in Fig. 3*A*) and an rms roughness of 1.1 nm. Finally, an AFM image of SCD reveals a surface that is almost atomically flat, with an rms T of only 0.18 nm. The angular features visible SCD surface in Fig. 3*A* are step edges that are a few atoms in height; the 60° angles of these edges confirm the (111) crystallographic orientation of the cleavage surface.

A comparison of the data before (Fig. 3 *A* and *B*) and after (Fig. 3 *C* and *D*) functionalization with EG6 (Fig. 3 *C* and *D*) shows that covalent functionalization with EG6 has little effect on the roughness. Small changes are observed that may arise from heterogeneity in the spatial distribution of EG molecules (leading to increased roughness) combined with the fact that flexible molecules may smooth out sharp gradients in height (leading to decreased roughness). However, the observed changes are small compared with the size of the avidin molecule. We showed previously that there is no detectable difference in grafting efficiency between NCD and SCD substrates (42). Consequently, we attribute any changes in protein binding between H-terminated and EG6-terminated surfaces to changes in the surface chemistry and not to changes in surface morphology or roughness.

Fig. 4 compares the roughness of the different surfaces (Fig. 4*A*) with the amount of avidin that nonspecifically binds (Fig. 4*B*). While the fluorescence measurements (together with standards of known concentration) directly yield the mass per unit area of adsorbed protein, by using the known dimensions of the avidin molecule (40 Å × 50 Å × 56 Å) (43) these data can be converted to a fractional monolayer coverage by assuming that avidin binds to the surface using the 40 Å × 50 Å face. Using this assumption, 100% monolayer equivalent (100% ML equ) corresponds to 8.3 pmol/cm^2. The data show that the H-terminated PD adsorbed the most avidin (43% ML equ, respectively), while the roughest surface, NCD, adsorbs only 3.3% ML equ. SCD (111) adsorbs the smallest amount, only 2.2% ML equ. After grafting of EG6 the nonspecific binding is again substantially reduced on all three types of diamond, but to varying degrees. Functionalization with EG6 reduces the adsorption of avidin on NCD by a factor of 1.7, while on PD nonspecific binding is reduced by a factor of 17, and on SCD it is reduced by a factor of 47.

The flattest sample, SCD, adsorbs only 3.9 ± 1.0 fmol/cm^2 or only 0.05% ML equ. of avidin. Surprisingly, however, while EG6-functionalized NCD has by far the roughest surface, it is much more effective than PD at resisting nonspecific binding of avidin. Thus, there is not a simple correlation between roughness and protein adsorption on a given surface.

Antibody-Modified Diamond Surfaces. The high chemical stability of diamond has been demonstrated previously when covalently linked to DNA oligonucleotides (22, 32) and when functionalized with EG oligomers for protein resistance (40). However, no previous study has examined stability of *proteins* covalently linked to diamond surfaces. Unlike DNA oligonucleotides that can be readily synthesized with well defined attachment points at one end, proteins have a more complex distribution of functional groups and are susceptible to changes in secondary and/or tertiary structure that may lead to loss of activity despite having no significant changes in primary structure (44).

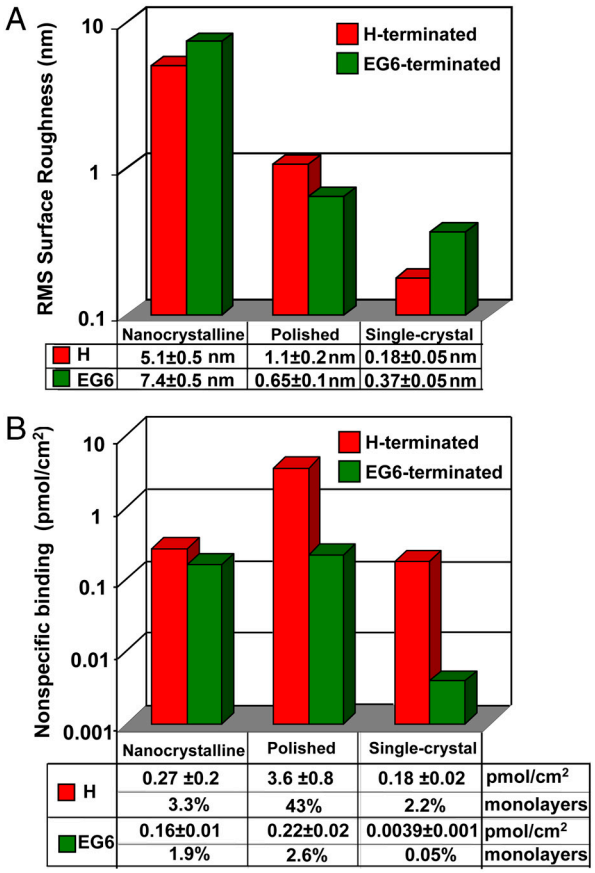

Fig. 4. *A*) rms roughness of diamond samples before and after functionalization with EG6. *B*) Amount of nonspecific binding of avidin on three types of diamond samples before and after functionalization with EG6.

To test whether photochemical grafting can yield increased chemical stability of protein-modified surfaces, we covalently grafted an antibody to the *Escherichia coli (E. coli)* K12 strain to diamond surfaces as depicted in Fig. 5 and used XPS to characterize the resulting changes in chemical structure. The most accessible functional groups for covalent attachment of antibodies are the amine groups that are prevalent in the F_{ab} region; unfortunately, this is also the region primarily responsible for molecular recognition. While attachment through the F_c region may be less disruptive to biological function, existing methods for covalent linking to the F_c region are harsh and may be disruptive to the antibody structure.(44, 45). Fig. 4 shows the approach we used here, in which glutaraldehyde is used as a bifunctional linker between the amine-terminated diamond surface and the free $-NH_2$ groups of the antibody (5, 23, 46).

We used XPS to investigate the chemical stability of *E. coli* antibodies covalently linked to diamond. For comparison, we also show similar results obtained using a commercially available glass substrate formed from γ-aminopropylsilane. In each case, an amine-terminated surface was prepared first, and then glutaraldehyde (followed by sodium cyanoborohydride) was used to link the amine-terminated surface to the free NH_2-groups of the antibody.

Fig. 6 shows XPS data of antibody-modified diamond and glass samples immediately after preparation and after storage for 14 d in phosphate-buffered saline solution at 37 °C. The C(1s) spectrum of the antibody-modified diamond samples show four peaks at 284.6 eV, 285.15 eV, 286.3, and 288.1 eV. These peaks arise from the diamond bulk (284.6 eV), alkyl carbons of the functionalization layer and of the protein (285.15 eV), and various forms of oxidized carbon including amides (286.2 eV) and carboxylic acids (288 eV). The N(1s) region shows a single sharp peak at 400 eV while the S(2p) region shows two peaks near 163 eV and 167 eV. XPS of functionalized glass surfaces are lower quality than those of diamond because of charging effects that broaden and shift the peaks. Nevertheless, Fig. 6 clearly shows that over the 14 d period of the experiment the C(1s) and N(1s) peaks decrease substantially while the intensity of the underlying silicon substrate Si(2s) peak increases. Sulfur(2p) peaks on glass are not visible because of their low intensity and charging effects.

Table 1 quantifies the relevant atomic ratios observed, represented as integrated peak area ratios after correction for the atomic sensitivity factors of the different elements. The most obvious difference is that the diamond surface shows no detectable change in the N(1s) signal, which arises primarily from the antibody. The change in Sulfur(2p) intensity on diamond is within the noise of the experiment (due to the intrinsically weak S(2p) intensity). In contrast, the glass surface loses 50% of nitrogen-bearing and carbon-bearing species over this same time period. Notably, however, both nitrogen and carbon decrease congruently, leaving the N/C ratio constant. From these data, we learn that the long-term stability of antibody-modified glass is significantly compromised by loss of the antibody from the surface, presumably through hydrolysis of the Si-O-C bonds at the antibody-glass interface. In contrast, the use of purely covalent chemistry leads to antibody-modified surfaces exhibiting higher chemical stability.

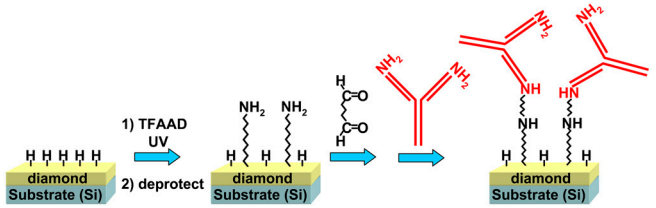

Fig. 5. Scheme for linking antibodies to diamond thin films.

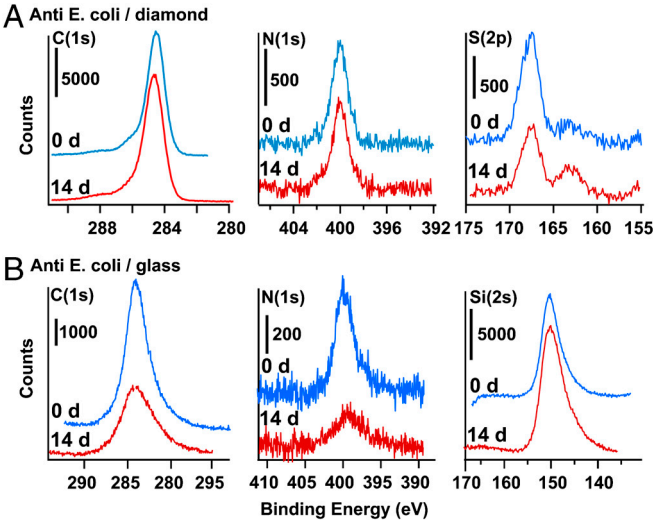

Fig. 6. XPS data depicting stability of anti-*E. coli* covalently grafted to amine-terminated diamond and amine-terminated glass substrates, and similar data after storage for 14 d in buffer solution at 37 °C. *A*) Carbon, Nitrogen, and Sulfur data for anti-*E. coli* on UNCD diamond thin-film. *B*) Carbon, Nitrogen, and Silicon data for anti-*E. coli* on glass.

To test whether the improved chemical stability of antibody layers on diamond results in a corresponding retention of biological activity, we conducted cell-capture studies on the above samples using the K12 serotype of *E. coli*. The number of cells captured per unit area on glass (N_{glass}) relative to that observed with UNCD (N_{UNCD}) shows that N_{Glass}/N_{UNCD} decreases from 0.84 on the freshly prepared surfaces (475 cells/mm^2 on UNCD and 400 cells/mm on glass, with a cell concentration of 5×10^7 colony-forming units per milliliter) to 0.45 (446 cells/mm^2 on UNCD, 204 cells/mm^2 on glass, 3.7×10^7 cfu/ml) on samples stored for 7 d at 37 °C. Thus, the greater stability of antibody-modified UNCD compared with that of glass observed in the XPS measurements is also reflected in improved retention of biological activity. These results suggest that antibody-functionalized diamond may be an excellent platform for selective capture of specific types of biological cells that may be of interest for water quality measurement or biological threat detection, as well as for controlling adhesion of cells for bioimplants and stem-cell research.

Discussion

Carbon-based materials hold enormous potential for the fabrication of highly stable molecular and biomolecular interfaces to biological systems. Prior studies using SAMs of thiolated ethylene glycol oligomers on gold (47–50) have found that the ability to resist protein binding depends strongly on the number density of the molecules (6, 13, 48–50). Determining the number density of EG molecules on diamond surfaces is challenging because carbon forms both the underlying substrate and the alkyl chain within the EG6 molecular layers. However, it is possible to estimate the number density because the EG6 molecules give rise to a unique peak near 286.6 eV binding energy from the C atoms that are adjacent to the O atoms in EG6 molecule (Fig. 2). Knowing that EG6 has 13 carbon atoms adjacent to O atoms and 10

Table 1. XPS measurements of chemical stability of anti-*E. coli*-modified diamond and glass surfaces

		$I_{Nitrogen}/I_{Carbon}$	I_{Sulfur}/I_{Carbon}	$I_{Nitrogen}/I_{Silicon}$	$I_{Carbon}/I_{Silicon}$
Glass	0 days			0.26	0.035
	14 days			0.13	0.018
Diamond	0 days	0.045	0.11		
	14 days	0.045	0.08		

atoms that are not, a more detailed peak area analysis allows us to establish the EG6 molecular layer has an area density of $\sim 2.6 \times 10^{14}$ molecules/cm^2, or 0.4 nm^2/molecule. This area per molecule is slightly larger than the value of 0.21 nm^2/molecule reported for a dense ethylene glycol SAM on Au, (49) but is within the range of values expected for a relatively dense SAM.

In contrast to a SAM on gold where lateral diffusion take place, grafting onto diamond and other covalent materials occurs more randomly on the surface, leaving small regions too small to accommodate molecules and resulting in a more open structure. This general picture has been confirmed on diamond through electrochemical measurements (5, 51). While a quantitative comparison is difficult, this analysis establishes that photochemical grafting yields layers with a density of exposed EG groups that is comparable to those produced by alkanethiols on gold.

Surface roughness is an important factor thought to influence the nonspecific binding of proteins. Yet, roughness is only a single measure of the topography of a surface, and despite many studies there appears to be no single unifying description of how roughness affects binding (1, 2, 52–54). Our experiments are performed on surfaces with rms roughness between 1.1 nm and 0.18 nm (PD and SCD), considerably smaller than the rms roughness in most other studies (53, 55). In addition, the length scale over which the roughness occurs may be important. We observe significantly more adsorption on the PD sample than on the NCD sample. Yet, closer examination shows that the NCD sample is comprised of crystalline grains that have smooth faces >30 nm in size, while the avidin protein is approximately 4 nm in size. Consequently, to a protein molecule this "rough" surface may appear locally smooth. In contrast, the polished sample has grooves that may be of the correct length scale to promote nonspecific binding through an increase in the interfacial contact area, likely driven by hydrophobic forces.

Finally, our results show that the outstanding performance of diamond as a substrate for biological studies can be extended to include antibody-modified surfaces. The XPS results presented here clearly show the improvement in chemical stability of the antibody-modified molecular layers and that this improvement in chemical stability is accompanied by an improvement in biological stability when used in cell-capture studies. Ultimately, it is likely that the long-term stability of proteins will be limited by changes in secondary and/or tertiary structure that will need to be addressed using other approaches.

Conclusions

These studies show that photochemical grafting of short ethylene glycol oligomers to diamond surfaces substantially reduces the nonspecific binding of proteins. XPS data show that grafting yields EG units whose density is comparable to that reported from EG-based self-assembled monolayers on gold. Despite having a modestly rough surface, a single molecular layer of EG6 on NCD reduces nonspecific binding to amounts that are undetectable by XPS, representing a residual nonspecific binding that is no more than 3% of that observed on the H-terminated surface. However, PD has significantly more nonspecific binding despite having a smaller rms roughness. Our results suggest that the lateral length scale is an important factor in determining how roughness impacts nonspecific binding of proteins on surfaces. Based on our data, we conclude that when surface features and proteins are similar in size, more protein will adsorb to those surfaces, likely as a direct result of the ability to achieve more direct contact area with the surface. Finally, our data show that the outstanding stability of carbon can be extended to antibodies, including improving the stability of surfaces designed to capture biological cells.

These results are significant from a biomaterials standpoint, since diamond and diamond-like carbon coatings have been used to increase biocompatibility (6, 7). Our results suggest that the use of molecular chemistry to modify the surface chemistry of diamond and diamond-like carbons may be beneficial in diverse applications ranging from diamond-like coatings on biomedical implants (56, 57) to the development of improved biosensors with improved longevity for applications such as continuous monitoring for *E. coli* and other biological pathogens.

While molecular layers on diamond are less structurally perfect than self-assembled monolayers on gold, alkanethiol SAMS are readily oxidized and not able to be easily integrated into more complex composite materials of importance in biomedical research (16, 52). In contrast, carbon represents a wide range of materials including diamond, amorphous carbon, tetrahedral amorphous carbon, and graphitic materials yielding a wide range of mechanical, optical, and electrical properties (58). The ability to fabricate highly stable, molecular and biomolecular layers on such materials represents an outstanding opportunity for biological surface chemistry in the years ahead.

Methods

Substrates and Sample Preparation. **NCD** 0.5 μm thick films grown on silicon were provided by the U.S. Naval Research Laboratory. UNCD samples, 1.0 μm thick on silicon substrates were grown by Advanced Diamond Technologies, Inc. Mechanically **PD** were **SCDs** with (100) surfaces fabricated by high-temperature, high-pressure synthesis by Sumicrystal Diamond. A single-crystal natural semiconducting type IIb SCD, cleaved along the (111) plane was provided on loan from the Naval Research Laboratory. Hydrogen-terminated diamonds were prepared by acid cleaning followed by exposure to a hydrogen plasma (36). Photochemical functionalization to graft molecular layers was performed by exposing the H-terminated surfaces to the neat liquid of the desired molecule(s) and illuminating with UV light (254 nm, 10 mW/cm^2) for 12 h (22). Resistance to nonspecific adsorption was conferred by binding vinyl-terminated oligo(ethylene glycol) monolayers to the surface. Hexaethylene glycol undec-1-ene (**EG6-ene**), was synthesized and fully characterized for these studies according to published procedures (15). Amine-terminated glass slides were Corning Gaps II Coated Slides, consisting of glass slides with a covalently bound coating of gamma-aminopropylsilanes.

X-Ray Photoelectron Spectroscopy. XPS measurements were performed in a custom-built XPS system using a Phi Al K_α source (1486.6 eV), an X-ray monochromator (excitation linewidth < 0.6 eV), and a hemispherical electron energy analyzer. C(1s) and N(1s) spectra were obtained using a 23.5 eV pass energy (0.35 eV resolution); S(2p) and Si(2s) spectra were obtained using a 117.4 eV pass energy (1.8 eV resolution).

AFM Measurements. Height images of each of the three diamond substrates were collected using tapping mode by a Digital Instruments Nanoscope IV microscope using a scan size of 2.0 μm.

Protein Adsorption and Wash-Off Measurements. For XPS studies of fibrinogen adsorption, diamond samples were incubated with ~0.2 mg/mL fibrinogen in 0.1 M $NaHCO_3$ (pH 8.3) for 1 h at room temperature. Rinsing followed, including an initial 15 min. soak in a wash-off buffer (pH 7.4) consisting of 0.3 M NaCl, 20 mM Na_2PO_4, 2 mM EDTA (commonly known as 2× Sodium Saline Phosphate Ethylenediamine tetraacetic acid (SSPE)) with 1% added Triton X-100, a second 5 min. soak in 2× SSPE, and two 5 min. soaks in deionized H_2O. Samples were dried and XPS measurements performed immediately.

For nonspecific binding measurements using avidin, fluorescein-labeled Avidin (Vector Labs) was diluted in 0.1 M $NaHCO_3$, pH 8.3, to 0.2 mg/mL concentration. Avidin solution was applied to the sample at room temperature for 1 h in a humidified chamber. The samples were rinsed and then soaked for 15 min in a wash-off buffer consisting of 2× SSPE with 1% Triton X-100. The remaining adsorbed protein was measured by digesting in a solution consisting of 1.00 mL of the wash-off buffer + 1% mercaptoethanol for 12 h; mercaptoethanol is a reducing agent that acts to cleave disulfide bonds in proteins, aiding their elution from the substrates into the elution buffer. The intensity of fluorescence at 518 nm (using 480 nm excitation) was measured.

Bacterial Cell Preparation and Capture Studies. Procedures followed for *E. coli* preparation and capture studies are described in *SI Text* on the PNAS web site, www.pnas.org.

ACKNOWLEDGMENTS. This work was supported in part by the National Science Foundation Grants CHE-0613010 and CHE-0911543, by the Defense Threat Reduction Agency (DTRA) under Contract HDTRA1-09-C-0007, and by the Naval Research Laboratory/Office of Naval Research.

1. Lord MS, Foss M, Besenbacher F (2010) Influence of nanoscale surface topography on protein adsorption and cellular response. *Nano Today* 5:66–78.
2. Boyan BD, et al. (2001) Mechanisms involved in osteoblast response to implant surface morphology. *Ann Rev Mater Res* 31:357–371.
3. Jon SY, et al. (2003) Construction of nonbiofouling surfaces by polymeric self-assembled monolayers. *Langmuir* 19:9989–9993.
4. Hartl A, et al. (2004) Protein-modified nanocrystalline diamond thin films for biosensor applications. *Nat Mater* 3:736–742.
5. Yang WS, Butler JE, Russell JN, Hamers RJ (2007) Direct electrical detection of antigen-antibody binding on diamond and silicon substrates using electrical impedance spectroscopy. *Analyst* 132:296–306.
6. Ostuni E, Yan L, Whitesides GM (1999) The interaction of proteins and cells with self-assembled monolayers of alkanethiolates on gold and silver. *Colloids and Surfaces B* 15:3–30.
7. Wisniewski N, Reichert WM (2000) Methods for reducing biosensor membrane biofouling. *Colloids and Surfaces B* 18:197–219.
8. Derda R, et al. (2010) High-throughput discovery of synthetic surfaces that support proliferation of pluripotent cells. *J Am Chem Soc* 132:1289–1295.
9. Hudalla GA, Murphy WL (2009) Using "click" chemistry to prepare SAM substrates to study stem cell adhesion. *Langmuir* 25:5737–5746.
10. Ivnitski D, Abdel-Hamid I, Atanasov P, Wilkins E (1999) Biosensors for detection of pathogenic bacteria. *Biosens Bioelectron* 14:599–624.
11. Wu GH, et al. (2001) Bioassay of prostate-specific antigen (PSA) using microcantilevers. *Nat Biotechnol* 19:856–860.
12. Castner DG, Ratner BD (2002) Biomedical surface science: foundations to frontiers. *Surf Sci* 500:28–60.
13. Ostuni E, Chapman RG, Holmlin RE, Takayama S, Whitesides GM (2001) A survey of structure-property relationships of surfaces that resist the adsorption of protein. *Langmuir* 17:5605–5620.
14. Sigal GB, Mrksich M, Whitesides GM (1998) Effect of surface wettability on the adsorption of proteins and detergents. *J Am Chem Soc* 120:3464–3473.
15. Pale-Grosdemange C, Simon ES, Prime KL, Whitesides GM (1991) Formation of self-assembled monolayers by chemisorption of derivatives of oligo(ethylene glycol) of structure $HS(CH_2)_{11}(OCH_2CH_2)_mOH$ on gold. *J Am Chem Soc* 113:12–20.
16. Flynn NT, Tran TNT, Cima MJ, Langer R (2003) Long-term stability of self-assembled monolayers in biological media. *Langmuir* 19:10909–10915.
17. Holmlin RE, Chen XX, Chapman RG, Takayama S, Whitesides GM (2001) Zwitterionic SAMs that resist nonspecific adsorption of protein from aqueous buffer. *Langmuir* 17:2841–2850.
18. Tidwell CD, et al. (1997) Endothelial cell growth and protein adsorption on terminally functionalized, self-assembled monolayers of alkanethiolates on gold. *Langmuir* 13:3404–3413.
19. Jans K, et al. (2008) Stability of mixed PEO-thiol SAMs for biosensing applications. *Langmuir* 24:3949–3954.
20. Robertson J (2002) Diamond-like amorphous carbon. *Mater Sci Eng R* 37:129–281.
21. May PW (2000) Diamond thin films: a 21st-century material. *Philos Trans R Soc Lond* 358:473–495.
22. Yang WS, et al. (2002) DNA-modified nanocrystalline diamond thin-films as stable, biologically active substrates. *Nat Mater* 1:253–257.
23. Sun B, et al. (2006) Covalent photochemical functionalization of amorphous carbon thin films for integrated real-time biosensing. *Langmuir* 22:9598–9605.
24. Wang X, Colavita PE, Streifer JA, Butler JE, Hamers RJ (2010) Photochemical grafting of alkenes onto carbon surfaces: identifying the roles of electrons and holes. *J Phys Chem C* 114:4067–4074.
25. Wang X, Ruther RE, Streifer JA, Hamers RJ (2010) UV-induced grafting of alkenes to silicon surfaces: photoemission vs. excitons. *J Am Chem Soc* 132:4048–4049.
26. Lasseter TL, Clare BH, Abbott NL, Hamers RJ (2004) Covalently modified silicon and diamond surfaces: resistance to nonspecific protein adsorption and optimization for biosensing. *J Am Chem Soc* 126:10220–10221.
27. Colavita PE, Sun B, Wang XY, Hamers RJ (2009) Influence of surface termination and electronic structure on the photochemical grafting of alkenes to carbon surfaces. *J Phys Chem C* 113:1526–1535.
28. Colavita PE, Sun B, Tse KY, Hamers RJ (2007) Photochemical grafting of n-alkenes onto carbon surfaces: the role of photoelectron ejection. *J Am Chem Soc* 129:13554–13565.
29. Lasseter TL, Cai W, Hamers RJ (2004) Frequency-dependent electrical detection of protein binding events. *Analyst* 129:3–8.
30. Baker SE, Colavita PE, Tse KY, Hamers RJ (2006) Functionalized vertically aligned carbon nanofibers as scaffolds for immobilization and electrochemical detection of redox-active proteins. *Chem Mat* 18:4415–4422.
31. Baker SE, et al. (2005) Covalent functionalization for biomolecular recognition on vertically aligned carbon nanofibers. *Chem Mat* 17:4971–4978.
32. Lu MC, et al. (2004) Invasive cleavage reactions on DNA-modified diamond surfaces. *Biopolymers* 73:606–613.
33. Sui JH, Cai W (2006) Effect of diamond-like carbon (DLC) on the properties of the NiTi alloys. *Diam Relat Mater* 15:1720–1726.
34. Shabalovskaya S, Anderegg J, Van Humbeeck J (2008) Critical overview of Nitinol surfaces and their modifications for medical applications. *Acta Biomaterialia* 4:447–467.
35. Baranauskas V, Fontana M, Guo ZJ, Ceragiolo HJ, Peterlevitz AC (2004) Analysis of the coagulation of human blood cells on diamond surfaces by atomic force microscopy. *Nanotechnology* 15:1661–1664.
36. Thoms BD, Owens MS, Butler JE, Spiro C (1994) Production and characterization of smooth, hydrogen-terminated diamond c(100). *Appl Phys Lett* 65:2957–2959.
37. Colavita PE, et al. (2008) Enhancement of photochemical grafting of terminal alkenes at surfaces via molecular mediators: the role of surface-bound electron acceptors. *J Phys Chem C* 112:5102–5112.
38. Nichols BM, Butler JE, Russell JN, Hamers RJ (2005) Photochemical functionalization of hydrogen-terminated diamond surfaces: a structural and mechanistic study. *J Phys Chem B* 109:20938–20947.
39. Ulman A (1996) Formation and structure of self-assembled monolayers. *Chem Rev* 96:1533–1554.
40. Clare TL, Clare BH, Nichols BM, Abbott NL, Hamers RJ (2005) Functional monolayers for improved resistance to protein adsorption: Oligo(ethylene glycol)-modified silicon and diamond surfaces. *Langmuir* 21:6344–6355.
41. Wagner MS, McArthur SL, Shen MC, Horbett TA, Castner DG (2002) Limits of detection for time of flight secondary ion mass spectrometry (ToF-SIMS) and X-ray photoelectron spectroscopy (XPS): detection of low amounts of adsorbed protein. *J Biomater Sci-Polym E* 13:407–428.
42. Nichols BM, et al. (2006) Electrical bias dependent photochemical functionalization of diamond surfaces. *J Phys Chem B* 110:16535–16543.
43. Pugliese L, Coda A, Malcovati M, Bolognesi M (1993) Three-dimensional structure of the tetragonal crystal form of egg-white avidin in its functional complex with biotin at 2.7 Å resolution. *J Mol Biol* 231:698–710.
44. Zhu H, Snyder M (2003) Protein chip technology. *Curr Opin Chem Biol* 7:55–63.
45. Nisnevitch M, Firer MA (2001) The solid phase in affinity chromatography: strategies for antibody attachment. *J Biochem Biophys Methods* 49:467–480.
46. Yang WS, Hamers RJ (2004) Fabrication and characterization of a biologically sensitive field-effect transistor using a nanocrystalline diamond thin film. *Appl Phys Lett* 85:3626–3628.
47. Prime KL, Whitesides GM (1993) Adsorption of proteins onto surfaces containing end-attached Olico(ethylene oxide): a model system using self-assembled monolayers. *J Am Chem Soc* 115:10714–10721.
48. Herrwerth S, Eck W, Reinhardt S, Grunze M (2003) Factors that determine the protein resistance of oligoether self-assembled monolayers—internal hydrophilicity, terminal hydrophilicity, and lateral packing density. *J Am Chem Soc* 125:9359–9366.
49. Harder P, Grunze M, Dahint R, Whitesides GM, Laibinis PE (1998) Molecular conformation in oligo(ethylene glycol)-terminated self-assembled monolayers on gold and silver surfaces determines their ability to resist protein adsorption. *J Phys Chem B* 102:426–436.
50. Unsworth LD, Sheardown H, Brash JL (2008) Protein-resistant poly(ethylene oxide)-grafted surfaces: chain density-dependent multiple mechanisms of action. *Langmuir* 24:1924–1929.
51. Tse KY, et al. (2005) Electrical properties of diamond surfaces functionalized with molecular monolayers. *J Phys Chem B* 109:8523–8532.
52. Nath N, Hyun J, Ma H, Chilkoti A (2004) Surface engineering strategies for control of protein and cell interactions. *Surface Sci* 570:98–110.
53. Han M, Sethuraman A, Kane R, Belfort G (2003) Nanometer-scale roughness having little effect on the amount or structure of adsorbed protein. *Langmuir* 19:9868–9872.
54. Xie HG, et al. (2010) Effect of surface morphology and charge on the amount and conformation of fibrinogen adsorbed onto alginate/chitosan microcapsules. *Langmuir* 26:5587–5594.
55. Muller B, et al. (2001) Impact of nanometer-scale roughness on contact-angle hysteresis and globulin adsorption. *J Vac Sci Technol B* 19:1715–1720.
56. Lappalainen R, Anttila A, Heinonen H (1998) Diamond coated total hip replacements. *Clin Orthop Rel R* 352:118–127.
57. Lappalainen R, Heinonen H, Anttila A, Santavirta S (1998) Some relevant issues related to the use of amorphous diamond coatings for medical applications. *Diam Relat Mater* 7:482–485.
58. Grill A (2003) Diamond-like carbon coatings as biocompatible materials—an overview. *Diam Relat Mater* 12:166–170.